Continuous-wave electromagnetically induced transparency: A comparison of V, Λ, and cascade systems

David J. Fulton,* Sara Shepherd, Richard R. Moseley, Bruce D. Sinclair, and Malcolm H. Dunn
J. F. Allen Physics Research Laboratories, Department of Physics and Astronomy, University of St. Andrews, North Haugh, St. Andrews, Fife KY16 9SS, Scotland, United Kingdom
(Received 27 February 1995)

A theoretical and experimental investigation has been carried out into the viability of V-type, Λ-type, and cascade systems within rubidium for the observation of electromagnetically-induced transparency (EIT). A Λ-type system is also discussed where EIT is induced on a two-photon transition. Continuous-wave single-frequency titanium sapphire lasers have been employed to provide the applied optical fields. It is found that systems that have a strong coupling field resonant with the $5S_{1/2}$ ground state suffer from complicating optical pumping mechanisms that tend to mask EIT windows. It is also found that wavelength matching of the applied optical fields enhances the observation of EIT since this results in a reduced residual Doppler linewidth of the atomic system.

PACS number(s): 42.50.Gy, 42.50.Hz, 32.80.Bx

I. INTRODUCTION

The effect termed electromagnetically induced transparency (EIT) is an induced transparency in an initially absorbing medium, experienced by a weak-probe field, due to the presence of a strong-coupling field on a linked transition. It was first theoretically discussed by Imamoğlu and Harris [1] and the first experimental observation of EIT was in neutral strontium by Boller, Imamoğlu, and Harris [2]. It has since been demonstrated that dc electric-field coupling can also produce this reduced absorption [3,4]. A major driving force behind the study of EIT is its application to the related topics of the enhancement of nonlinear wave-mixing process [5,6], systems that provide lasing without a population inversion [7] (and references therein), and for the generation of phaseonium-type media [8,9]. The observation of sub-Doppler continuous-wave EIT has also been carried out by various groups [10–12]. A continuation of the theoretical work on EIT has resulted in proposals for induced phase matching [13], matched pulse effects [14], and normal modes or dressed-field pulses for EIT [15,16].

In this paper we investigate, both theoretically and experimentally, EIT produced in three popularly discussed system shown schematically in Fig. 1. This allows a comparison of the three EIT systems to be made, including a discussion of the experimental practicalities of each system for further experimental work.

The first, Fig. 1(a), is termed a V-type system. An initial theoretical and experimental comparison between V-type EIT coherent population trapping, and multilevel optical pumping has previously been discussed by Weiss, Sander, and Kanorsky [17]. They employed continuous-wave diode lasers to produce their coherent electromagnetic fields with output powers of ~10 mW. More recently, a V-type system has been employed within a potassium-helium mixture to produce steady-state gain [18]. Our second scheme is the so-called Λ-type system, Fig. 1(b). This scheme was employed by Gray, Whitley, and Stroud in their studies of coherent trapping of atomic populations [19]. They viewed this coherent population trapping as a problematic feature to be circumvented so as to enable maximum extraction of the ground-state population. Extensive theoretical work has since been carried out on these Λ-type systems [20,21]. The first successful EIT experiment in fact employed a Λ-type system and pulsed lasers [2]. In addition, a continuous-wave coherence experiment was carried out on a Λ-type sys-

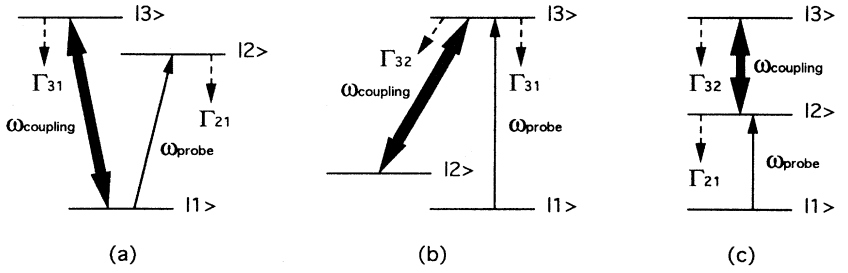

FIG. 1. Schematic energy-level diagrams showing the ideal three-level atoms, with the relevant population decay values (Γ_{ij}), the probe field transitions (ω_p), and the coupling field transitions (ω_c) for (a) the V-type system, (b) the Λ-type system, and (c) the cascade system.

*Electronic address: djf1@st-and.ac.uk

tems by Akulshin, Celikov, and Velichansky [22]. Although these authors were observing coherent population trapping effects, their experiments show distinctive EIT features. However, this work was prior to the first discussion of EIT by Harris and co-workers [1,2,23]; thus the connection to EIT and its terminology, was not made. Initially we consider the suitability of a similar Λ-type system to that considered by the above authors for the observation of EIT [19,22]. A second Λ-type system involving a two-photon probe field is then examined. The final scheme to be examined is termed a cascade system, shown in Fig. 1(c). This system was first shown to be experimentally viable by Field, Hahn, and Harris [23] when lead vapor was rendered transparent by the application of pulsed laser sources. Moseley *et al.* have carried out extensive, continuous-wave, theoretical and experimental work on this system [12,24]. The effect that an applied magnetic has on an EIT window within a cascade system has also recently been studied [25]. This paper highlights some important characteristics of the cascade system so allowing a comparison of the three schemes to be made.

II. RESIDUAL DOPPLER LINEWIDTHS

Although continuous-wave lasers may not provide the powers to produce Autler-Townes splitting greater than the inherent single-photon Doppler linewidths of the interaction medium, EIT can be observed as long as the Autler-Townes splitting is greater than the residual two-photon linewidth of Doppler reduced experiments [10,24]. The residual Doppler linewidth (in hertz) $\Delta\nu_D$ of an EIT system is given by the expression

$$\Delta\nu_D = |(k_1 \pm k_2)|u \ , \tag{1}$$

where k_i is the wave number of the applied optical field, which takes a positive value if propagation is in the positive z direction or a negative value if oriented in the opposite sense. The negative sign in Eq. (1) corresponds to V-type and Λ-type systems, while the positive sign is for cascade systems. The value of u is given by

$$u = \left[\frac{2k_B T}{M}\right]^{1/2} , \tag{2}$$

where k_B is the Boltzmann constant, T the temperature of the gas in Kelvin, and M the atomic mass. Thus, if the coupling field Rabi frequency is greater than the residual Doppler linewidth, then good EIT is observed.

III. THEORETICAL IDEAL THREE-LEVEL SYSTEMS

Our experiments deal with coherent effects induced on atoms due to applied optical fields, produced by employing continuous-wave lasers. Thus, using a density matrix formalism, a theoretical analysis of these steady-state conditions can be carried our in a fashion similar to that used by Brewer and Hahn [26]. By way of introduction, a simplified theoretical analysis is presented here, where we have assumed that (i) the three atomic systems are homogeneous, i.e, we neglect the effects of Doppler broadening, (ii) all dipole-allowed transitions have equal population decay rates (to which the coherence dephasing rates are directly related) and equal dipole transition matrix elements; and (iii) all dipole-forbidden transitions have zero-valued population decay rates. In each system the coupling field is set to induce a Rabi frequency of 10 MHz, the probe field is set to induce a Rabi frequency of 1 MHz on their respective transitions, and all nonzero population decay rates Γ_{ij} are set to 10 MHz. With these assumptions the coherence dephasing rates of the dipole-forbidden transitions are (referring to Fig. 1)

$$\gamma_{23} = \frac{\Gamma_{21}}{2} + \frac{\Gamma_{31}}{2} \quad (\text{V}-\text{type system}) , \tag{3}$$

$$\gamma_{12} = 0 \quad (\Lambda-\text{type system}) , \tag{4}$$

$$\gamma_{13} = \frac{\Gamma_{32}}{2} \quad (\text{cascade system}) . \tag{5}$$

The strength of an EIT window is strongly dependent on the coherence dephasing rate of the dipole-forbidden transition. Therefore it is expected that, with all the other parameters being equal, the ideal Λ-type system will produce the best EIT window and the ideal V-type systems the poorest. However, EIT is not the only source of increased transparency in these ideal models. Within the V-type system, EIT cannot be isolated from an increased probe field transmission, induced by the coupling field saturating the $|1\rangle$-$|3\rangle$ transition. Also the Λ-type system is complicated by population being optically pumped into level $|2\rangle$ by the probe field. However, population trapped due to optical pumping, within the Λ-type system, is normally reduced by the presence of the coupling field since it acts to repump population out of level $|2\rangle$ back into the system. Thus the presence of a coupling field causes the maximum absorption experienced by the probe field, in a Λ-type system, to be enhanced.

Three different curves, for each system, have been generated from these ideal three-level models and are shown in Fig. 2. In this figure the imaginary component of ρ_{12}, which is directly related to the absorption experienced by the probe field, has been plotted against the detuning of the probe field. The solid lines show the absorption line shapes generated for each system, in the presence of all the induced transparency mechanisms. The greatest transparency depth can be seen to occur in the Λ-type system and is simply due to the effect of EIT. However, the V-type system is seen to produce a transparency window of greater depth than the cascade system since this window is a result of the combination of EIT and coupling field saturation. The EIT windows can be artificially removed by increasing the dephasing rate on the uncoupled transition in each system. This is achieved by adding a constant dephasing rate term of 10 GHz to Eqs. (3)–(5). Three curves incorporating this change are represented by the doted lines marked with crosses in Fig. 2. It is seen that the maximum absorption of the probe field in the V-type and Λ-type system is less than in the cascade system due to coupling field saturation effects and population trapping within level $|2\rangle$, respectively. A more realistic alteration to the ideal models is to dephase

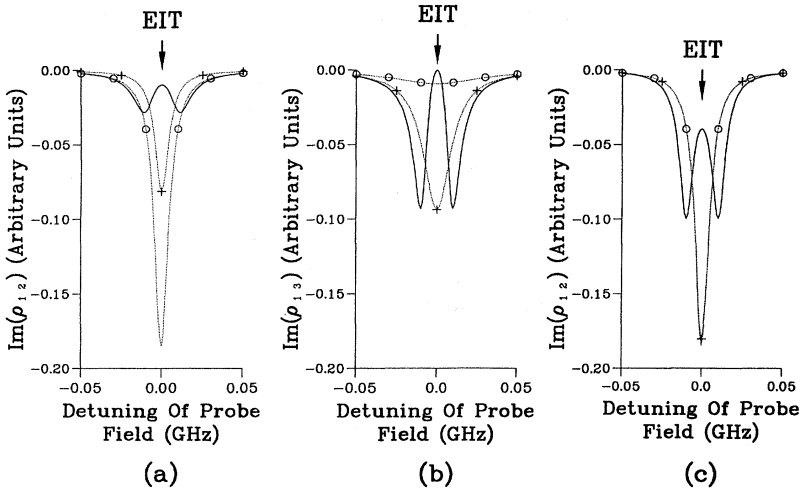

FIG. 2. Im(ρ_{12}) (proportional to probe field absorption) versus the detuning of the probe field for the ideal three-level V-type, Λ-type, and cascade systems, with a probe field Rabi frequency of 1 MHz and a coupling field Rabi frequency of 10 MHz. All the nonzero population decay rates are set to be 10 MHz. Solid lines show absorption line shapes including EIT. Dotted lines marked with crosses are those with 10-GHz constant dephasing rate terms added to the uncoupled transitions. Dotted lines marked with circles are those with 10-GHz constant dephasing rate terms added to both uncoupled and coupling field transitions.

particular levels rather than just single transitions, i.e., level $|3\rangle$ in the V-type and the cascade system and level $|2\rangle$ in the Λ-type system. This results in the dephasing of all the coherence terms related to this level and so the coupling field transition as well as the uncoupled transition must be artificially dephased. This is the case represented by the dotted lines marked by circles in Fig. 2. By increasing the dephasing rate on the coupling field transition we effectively reduce the interaction between this optical field and the atom. Thus the effects of coupling field saturation within the V-type system and optical repumping within the Λ-type system are reduced by increasing the related dephasing rate. An analysis of the density matrix equations used to derive our model of three-level atom reveals that an artificial increase of the dephasing rate on the coupling field transition produces the same effect as a reduction of the power of the coupling field.

In practice, a complete comparison between the three schemes is hindered because three systems with identical atomic parameters do not exist. For this reason, population decay rates, coherence dephasing rates, and dipole matrix elements between levels $|1\rangle$, $|2\rangle$, and $|3\rangle$ for each system of Fig. 1 will vary, affecting the EIT realized in each. Also the energy levels involved with the dipole-forbidden transitions can never have zero-valued population decays rates. This is because these forbidden lines may still occur through non-electric-dipole transitions and further dephasing may be induced through collision mechanisms [27]. Interaction with only three levels within an atomic structure is itself difficult because each level has an associated structure. It is found that optical pumping between hyperfine ground states greatly complicates the interpretation of experimental results within the V-type and Λ-type systems. However, by varying the experimental procedures between systems, these complicating optical pumping characteristics can be circumvented. A further limitation of our ideal three level models is the assumption that the levels are purely homogeneously broadened. Our experiments are carried out in vapor cells and so inhomogeneous Doppler broadening of the systems is experienced. The effects of Doppler broadening can be reduced by careful experimental planning. As discussed in Sec. II, the basic requirement is that the residual Doppler linewidths of the experiment are less than the induced Autler-Townes splitting. This results in a reduced power threshold requirement on the coupling field Rabi frequency such that EIT can be physically observed. All these factors are taken into account when discussing the practicalities of each system for further experimental work.

IV. EXPERIMENTAL APPARATUS

The apparatus used in this experiment is similar to that of previously reported work [12,24,25]. Optical fields were produced by two single-frequency, linearly polarized, continuous-wave Ti:sapphire ring lasers, pumped by separate mainframe argon-ion lasers. The scanning optical field source was produced by a Microlase MBR-110 Ti:sapphire laser, while the nonscanning source was provided by a modified Schwartz Electro-Opti Titan Ti:sapphire laser [28]. Measurements on the Schwartz nonscanning laser indicated a linewidth and drift of approximately 5 MHz over the time of one scan of the Microlase laser. The choice of which laser provided the probe optical field and which the coupling optical field depended on what system was being studied. Wavelengths as well as probe and coupling fields orientations were also system dependent and are described for each system in Secs. V, VI, and VII, respectively. The probe field was usually attenuated via neutral density filters to ≤ 50 μW (with a minimum waist of 100 μm in the cell) to avoid saturation and self-focusing effects. The coupling laser provided up to 600 mW of power and was focused to a minimum waist of 150 μm in the cell. It was, however, attenuated via neutral density filters to ~ 5 mW for the V-type and Λ-type systems since power broadening hindered the interpretation of these experimental results. The two laser fields were linearly polarized in the same plane, except for the case of the Λ-type system experiments. Here the wavelengths of the applied optical field were so close that orthogonally polarized lasers fields have to be employed so as to avoid the coupling field

flooding the probe field at the detector. Orthogonal polarization of the laser fields was achieved by rotating the coupling field with a half wave plate. The coupling field was then filtered out before reaching the detector by the use of linear polarizing cubes. The filtering out of the coupling field in the V-type system experiments could be done by simply employing a rubidium D_1 or D_2 line interference filter.

The rubidium vapor was contained within a 10-cm-long quartz cell at a temperature of 45 °C providing a density of 10^{17} atoms/m^3. When the beams were focused, lenses were chosen such that the confocal parameters for both fields matched the length of the vapor cell and the probe field propagated within the spatial profile of the coupling field. For the V-type and Λ-type systems the laser fields co-propagated through the cell, whereas they counter-propagated for the cascade system experiments so as to minimize the residual Doppler linewidths. The probe field was detected by a large-area photodiode in all three systems in order to avoid the effects of electromagnetically induced focusing [12]. For the cascade and two-photon Λ-type systems a 422-nm fluorescence signal ($6P$-$5S_{1/2}$) was also monitored from the top of the rubidium cell, using a filtered photomultiplier tube (R.C.A. IP28, with Schott Glasses BG38 filters). This signal monitored the population of the $5D_{5/2}$ level via cascade decay. Phase-sensitive detection was used for both of these diagnostic signals to raise the signal-to-noise ratio. Single-mode operation was monitored by 1.5-GHz confocal étalons and absolute wavelengths were measured by a Kowalski-style traveling wave meter.

V. V-TYPE SYSTEM

The V-type system used for this theoretical and experimental study employs the D_1 line (794 nm) and D_2 line (780 nm) of rubidium, as shown in Fig. 3. The energy level structure of ^{87}Rb is shown in Fig. 3(a) and that of ^{85}Rb in Fig. 3(b). Both of these systems are studied experimentally in order to test our theoretical predictions. Our experimental analysis of a V-type system is carried out by scanning the frequency of the coupling field, while employing a static frequency probe field as described by Weiss, Sander, and Kanorsky [17]. Here the coupling field is focused using a 40-cm lens and is scanned upward in frequency across the $5S_{1/2}$-$5P_{3/2}$ transition while the probe laser is focused with a 50-cm lens and set on the $5S_{1/2}$-$5P_{1/2}$ transition. Copropagating laser beams are used so as to reduce the effective residual Doppler linewidth. For this system the employment of Eq. (1) results in a value for the residual Doppler linewidth of ~6 MHz. The effect on the transmission of the probe field due to the scanning coupling field is monitored.

In Fig. 4 we provide schematic diagrams showing the four simultaneously occurring mechanisms present in this V-type system. A detailed analysis of this system can be found in Ref. [17]; however, for the purpose of this paper we provide a brief overview of these four mechanisms. Mechanism 1, shown in Fig. 4(a), is the V-type system required for the observation EIT. The system for coupling field saturation, termed mechanism 2, is represented in Fig. 4(b). Here the coupling field causes a distribution of the population between levels $|1\rangle$ and $|3\rangle$, as described in Sec. III. A further complicating factor, which can also act to mask the observation of EIT in this V-type system, is optical pumping. There are in fact two velocity selective optical pumping mechanisms in our V-type system. The first, mechanism 3, involves optical pumping between ground-state hyperfine levels, as shown in Fig. 4(c). Atomic selection rules for electric-dipole-allowed transitions are that $\Delta F=0,\pm1$ for both excitation and decay [27]. Thus, for example, with an initial ground-state level of hyperfine quantum number F, optical pumping into the $F-1$ ground state occurs if level $|3\rangle$ has a hyperfine quantum number F or $F-1$. However, this optical pumping mechanism is not 100% efficient due to a collisional and thermal redistribution of the population within the ground-state hyperfine levels. The second optical pumping mechanism, termed mechanism 4, occurs between magnetic hyperfine sublevels [29]. This is only distinguishable when the coupling field is resonant with an $(F)|1\rangle$-$(F+1)|3\rangle$ transition and the probe field is simultaneously resonant with an $(F)|1\rangle$-$(F-1)|2\rangle$ transition, shown schematically in Fig. 4(d). Effectively the coupling field pumps population to lower $|m_F|$ valued hyperfine ground states, thus producing an increased absorption on the probe field due to the increased ground-state population available.

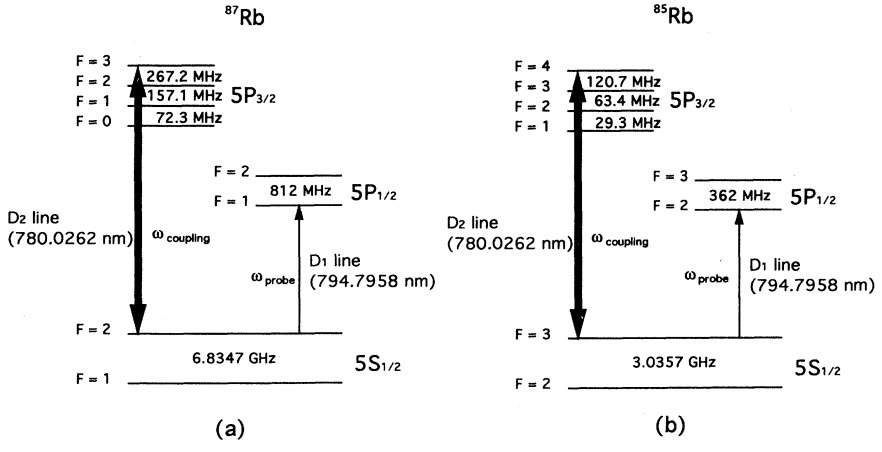

FIG. 3. Partial energy-level diagram of rubidium showing the scheme employed for the V-type system experiment within (a) the ^{87}Rb isotope and (b) the ^{85}Rb isotope.

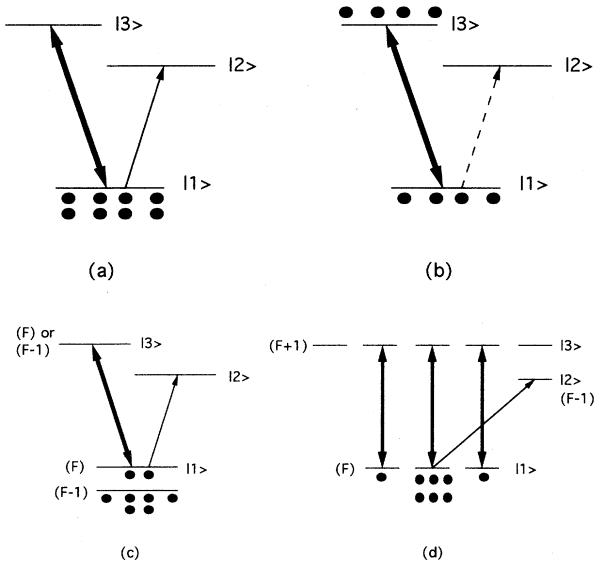

FIG. 4. Schematic diagrams representing the four simultaneously occurring mechanisms in this V-type system: (a) mechanism 1, V-type system required for the observation of EIT; (b) mechanism 2, coupling field saturation; (c) mechanism 3, optical pumping between ground state hyperfine levels; (d) mechanism 4, optical pumping between magnetic hyperfine sublevels. Two-headed arrows represent the coupling field while single headed arrows the probe field.

In Fig. 5 we present an experimental trace of the probe field transition versus the scanning of the coupling field for ^{85}Rb. The first cluster of three peaks corresponds to the case where the probe field is velocity selected into resonance with the $5S_{1/2}(F=3)$-$5P_{1/2}(F=3)$ transition, while the coupling field is scanned upward in frequency across the $5S_{1/2}(F=3)$-$5P_{3/2}$ transition. The probe field is then velocity selected into resonance with the $5S_{1/2}(F=3)$-$5P_{1/2}(F=2)$ transition as the coupling field continues to scan and so produces the second cluster of three peaks. The four peaks marked by a vertical line correspond to the case when mechanisms 1–3 are present. The contributions of all these mechanisms act to increase the transmission of the probe field and as a result EIT cannot be resolved. The peak marked by the tailed arrow comprises of mechanisms 1 and 2. Again both act to increase the probe field transparency and so EIT cannot be resolved, but this increase is not as large as the previous case since no optical pumping between the ground-state hyperfine levels is present. The final peak, marked by a nontailed arrow, consists of mechanisms 1 and 2, which act to increase the probe field transmission, and mechanisms 4, which acts to reduce it. Thus the coupling field saturation effect and EIT appear imprinted on a reduced transparency background. It has been pointed out by Weiss, Sander, and Kanorsky [17] that this transparency window cannot solely be accounted for by coupling field saturation since its depth is much greater than would be expected for this process alone. The increased transparency depth is thus EIT: a reasonably arrow, 35-MHz, feature that clearly increases the transmission of the probe field.

In Fig. 6 three probe field transmission traces for ^{87}Rb are presented, where the coupling field has been quartered in power between each trace. Quartering the power corresponds to halving the Rabi frequency. Thus the combined EIT and coupling field saturation feature, whose frequency position is marked by an arrow, should reduce in width by around a factor 2 between each trace.

A point to note is that EIT can never be distinguished from optical pumping if the two optical fields are swapped over such that the scanning coupling field is on the $5S_{1/2}(F=3)$-$5P_{1/2}$ transition and the probe field on the $5S_{1/2}(F=3)$-$5P_{3/2}$ transition. Optical pumping between the hyperfine ground states, mechanism 3, can never be eliminated in this system and so EIT will always be masked by this effect. An experimental curve, shown in Fig. 7 for ^{87}Rb, confirms this point. The trace shows

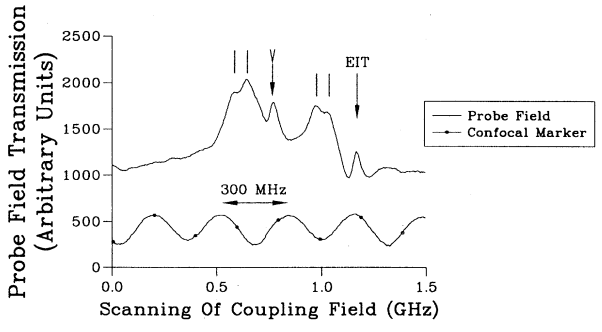

FIG. 5. Probe field transmission recorded versus the scanning of the coupling field for the ^{85}Rb V-type system experiment. Vertical lines mark the frequency position of peaks dominated by mechanism 3. The tailed arrow marks the frequency position of peak 3, which does not suffer from the effects of mechanism 3. The nontailed arrow marks the frequency position of the EIT feature. A 300-MHz confocal signal is also present as a frequency reference.

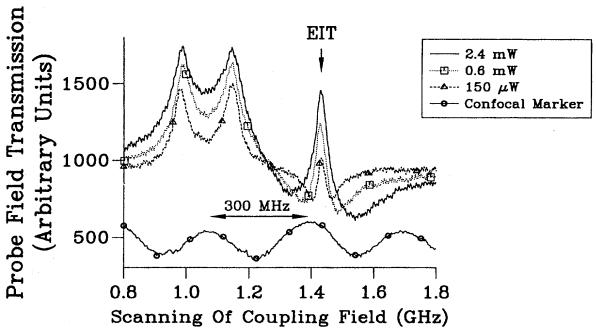

FIG. 6. Three probe field transmission curves recorded versus a scan of the coupling field for an ^{87}Rb, V-type system experiment. The probe field is set on the $5S_{1/2}(F=2)$-$5P_{1/2}$ transition while the coupling field is scanned across the $5S_{1/2}(F=2)$-$5P_{3/2}$ transition. The frequency position of the three EIT features is marked by an arrow. A 300-MHz confocal signal is also present as a frequency reference.

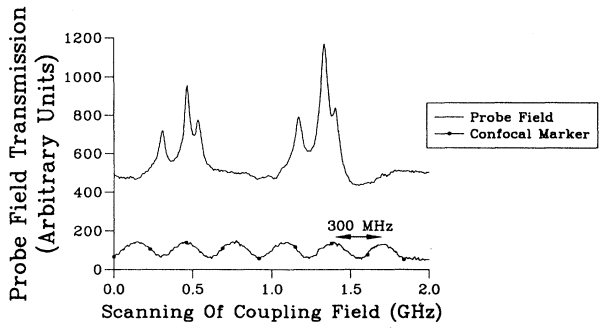

FIG. 7. Probe field transmission curve recorded versus a scan of the coupling field for an ^{87}Rb V-type system experiment. The probe field is set on the $5S_{1/2}(F=2)$-$5P_{3/2}$ transition while the coupling field is scanned across the $5S_{1/2}(F=2)$-$5P_{1/2}$ transition. The coupling field has a power of 165 mW. A 300-MHz confocal signal is also present as a frequency reference.

strong optical pumping features on all six peaks that act to mask any EIT. Again the structure of the $5P_{3/2}$ and $5P_{1/2}$ levels can be clearly resolved.

VI. Λ-TYPE SYSTEM

Two different Λ-type systems have been studied in this paper. The first system has a single-photon probe field set on the $5S_{1/2}$-$5P_{1/2}$ transition, whereas the second system employs a two-photon probe field resonant with the $5S_{1/2}$-$5D_{5/2}$ transition. We shall take both systems in turn and discuss the feasibility of each for observing EIT.

A. A Λ-type system employing a single-photon probe field

This Λ-type system is based on the D_1 line of ^{85}Rb, $5S_{1/2}$-$5P_{1/2}$. The energy level configurations involved in this system are shown in Fig. 8. The probe field is set to be resonant with the $5S_{1/2}(F=2)$-$5P_{1/2}$ transitions, while the coupling field is scanned across the $5S_{1/2}(F=3)$-$5P_{1/2}$ transition. It should be noted that the frequency separation of the $5P_{1/2}$ hyperfine levels, 362 MHz, is not sufficient to allow either of these levels to be isolated as the upper state for our Λ-type system. The optical fields are unfocused and copropagate so as to reduce the residual Doppler linewidth to a value of 2.5 kHz. Since our coupling field is resonant with a ground-state level it is expected that strong optical pumping will be experienced between the ground-state hyperfine levels, in a similar fashion to that seen in the V-type system. A four-level density matrix analysis has been carried out on this Λ-type system and is represented in Fig. 8. Shown in Fig. 8(a) is a theoretical trace of the probe field transmission versus coupling field detuning. This curve can be seen to consist of three reduced transmission components, separated by 362 MHz. The middle feature consists of a combination of optical pumping, between the ground-state hyperfine levels, and EIT. This corresponds to the case represented in Fig. 8(c), where both of the optical fields are simultaneously velocity shifted into resonance with the same upper state $5P_{1/2}$ hyperfine levels, thus producing EIT. This occurs when the applied optical fields are separated in frequency by the splitting of the ground-state levels. The other two reduced transmission features arise from simultaneous velocity shifts of both

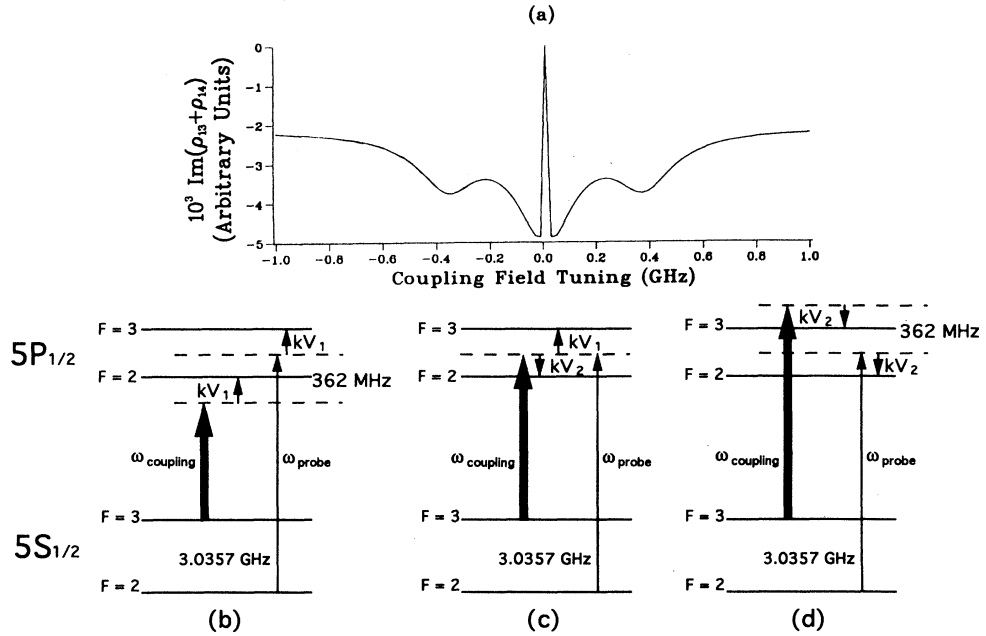

FIG. 8. (a) Im($\rho_{13}+\rho_{14}$) (proportional to probe field absorption) versus the detuning of the coupling field for the single-photon Λ-type systems within ^{85}Rb vapor, with a probe field Rabi frequency of 1 MHz on the $5S_{1/2}(F=2)$-$5P_{1/2}$ transition, and a coupling field Rabi frequency of 20 MHz on the $5S_{1/2}(F=3)$-$5P_{1/2}$ transition. The three observed probe field transmission features correspond to the partial energy diagrams shown in (b)–(d), respectively.

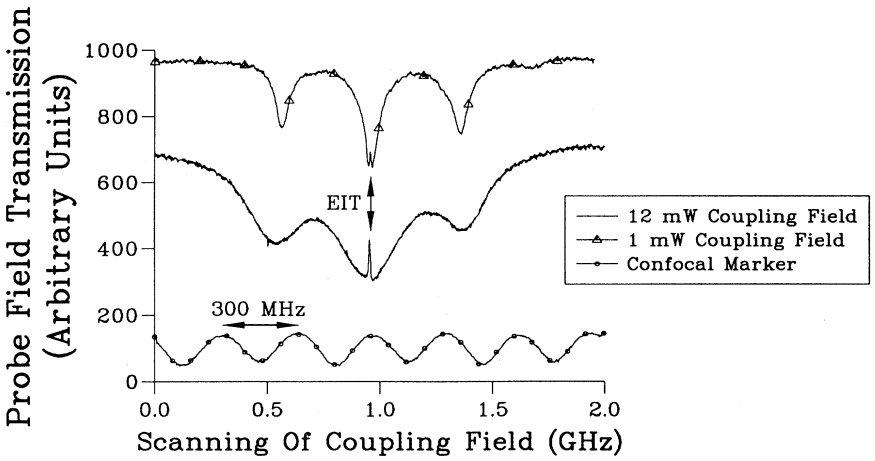

FIG. 9. Two probe field transmission curves recorded versus a scan of the coupling field for the ^{85}Rb, single-photon probe Λ-type system experiment. The probe field is set on the $5S_{1/2}(F=2)$-$5P_{1/2}$ transition while the coupling field is scanned across the $5S_{1/2}(F=3)$ -$5P_{1/2}$ transition. The frequency position of the two EIT features is marked by a double-headed arrow. A 300-MHz confocal signal is also present as a frequency reference.

optical fields onto different upper-state hyperfine levels [Figs. 8(b) and 8(d)]. Since the two optical fields no longer share a common upper level, the conditions for EIT are not met and so the transmission features consist simply of optical pumping between ground-state hyperfine levels.

Experimental traces of the probe field transmission versus the coupling field detuning are shown in Fig. 9. The two traces differ in the fact that the coupling field is a factor 10 greater in the second trace than in the first. Our three predicted reduced probe transmission features, with EIT imprinted on the second, can clearly be seen on both traces. The degree of optical pumping and the depth of the EIT window can be seen to fall off with the power reduction of the coupling field.

B. A Λ-type system employing a two-photon probe field

The second Λ-type system studied is based on the $5S_{1/2}$-$5P_{3/2}$-$5D_{5/2}$ scheme within rubidium. These energy levels are employed as a Λ-type system by setting the coupling field on the $5P_{3/2}$-$5D_{5/2}$ transition while employing a two-photon scanning probe field on the $5S_{1/2}$-$5D_{5/2}$ transition. This two-photon probe field is employed so as to provide a Λ-type system that does not have the coupling field resonant with the ground state and thus does not suffer from optical pumping between ground-state hyperfine levels. In this experiment the incoherent fluorescence from the $6P$-$5S_{1/2}$ transition is monitored at right angles to the direction of the laser beams. This fluorescence is directly proportional to the population present in the $5D_{5/2}$ level. We infer the presence of EIT through observation of dips in the fluorescence signal. This scheme, with the appropriate optical field wavelengths, is shown in Fig. 10.

The important factor in this Λ-type system for observing EIT is the linewidth of the uncoupled $5S_{1/2}$-$5P_{3/2}$ transition. Copropagating fields cause the two-photon transition to be Doppler broadened, but still provides a residual Doppler linewidth of ~710 MHz. With this probe field orientation it proved possible to observe dips in the fluorescence signal, thus inferring the presence of EIT, shown by the experimental traces of Fig. 11. The transparency window observed in this system is relatively broad, 300 MHz, and not of any great depth, ~10%. This width is the result of EIT windows at slightly different frequency positions due to the various velocity groups coming into two-photon resonance with each of the hyperfine levels in the $5P_{3/2}$ state. A restriction on the strength to the EIT window in this system is the fact that the uncoupled transition is in fact dipole allowed and so will inherently produce strong dephasing of this transition. Also included in Fig. 11 is the $6P$ fluorescence signal in the absence of the coupling field (triangle marked line). Here it is seen that the maximum fluorescence is significantly less than for the case where the coupling field is present. The reason for this is that the population of the $5D_{5/2}$ level can decay to the $5S_{1/2}$ ground state by employing either the $6P$ or the $5P_{3/2}$ level as an intermediate state. Now, with the coupling field on, any population that decays into the $5P_{3/2}$ level is quickly reexcited back to the $5D_{5/2}$ level. Thus the preferential decay route is the one involving the $6P$ level and so the fluorescence signal is increased in the presence of the coupling field.

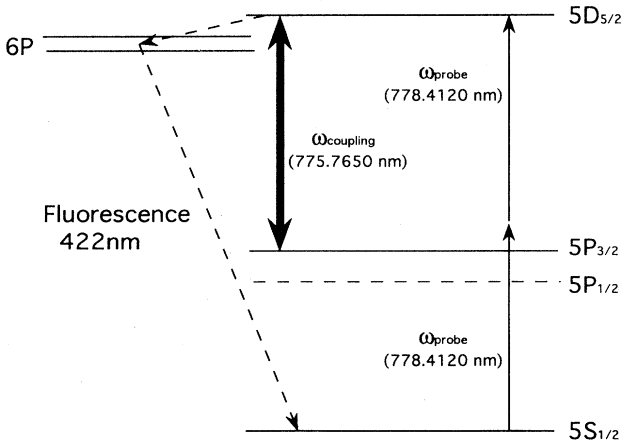

FIG. 10. Partial energy-level diagram of rubidium showing the scheme employed for the two-photon probe Λ-type system experiment.

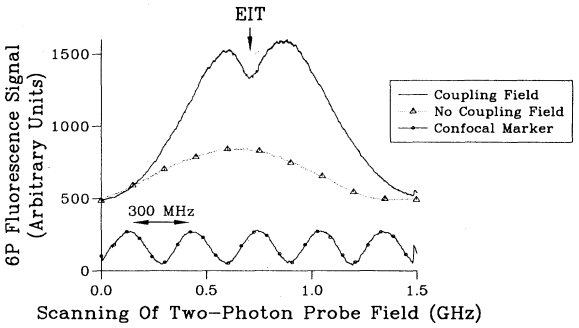

FIG. 11. $6P$ (422 nm) fluorescence signal curve recorded versus a scan of the two-photon probe field, for ^{85}Rb, in the two-photon probe Λ-type system experiment. Fluorescence with coupling field, $\sim$300 mW, present is represented by the solid line and absent by the triangle marked line. The two-photon probe field is scanned across the $5S_{1/2}(F=3)$-$5D_{5/2}$ transition while the coupling field is resonant with the $5P_{3/2}$-$5D_{5/2}$ transition. The frequency position of the EIT features is marked with an arrow. A 300-MHz confocal signal is also present as a frequency reference.

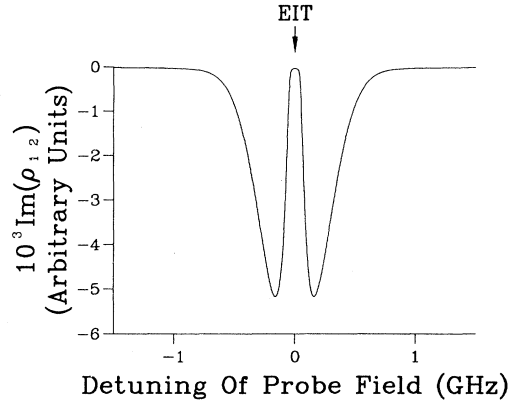

FIG. 13. Im(ρ_{12}) (proportional to probe field absorption) versus the detuning of the probe field, for ^{85}Rb vapor, within the cascade system. The frequency position of the EIT window is marked by an arrow. There is a probe field Rabi frequency of 1 MHz on the $5S_{1/2}$-$5P_{3/2}$ transition and a coupling field Rabi frequency of 160 MHz on the $5P_{3/2}$-$5D_{5/2}$ transition.

The normal orientation for two-photon spectroscopy experiments is that the two-photon transition is induced by the interaction of two counterpropagating photons [30]. With counterpropagating probe field photons all the atomic velocity groups are simultaneously resonant with the two-photon transition; hence this transition is termed Doppler free. This, like the previous copropagating system, provides a residual Doppler linewidth of $\sim$710 MHz. So far, however, we have been unable to observe EIT with this arrangement for reasons not yet clear to us.

VII. CASCADE SYSTEM

The cascade system studied here employs the $5S_{1/2}$-$5P_{3/2}$-$5D_{5/2}$ energy levels within rubidium as shown in Fig. 12. A scanning probe field is resonant with the $5S_{1/2}$-$5P_{3/2}$ transition, while a coupling field of fixed frequency is resonant with $5P_{3/2}$-$5D_{5/2}$ transition. EIT is observed in this system by monitoring the probe field transmission. The residual Doppler linewidth is reduced to $\sim$1.65 MHz in this system by employment of a counterpropagating field geometry. Both lasers are focused into the 10-cm-long rubidium cell, the coupling field by a 50-cm lens, and the probe field by a 40-cm lens. This system does not involve complicating optical pumping mechanisms since the coupling field is not resonant with the ground state and, by definition, the probe field is of low enough power such that it does not produce large-scale population movement.

A theoretical prediction for the observation of EIT within this system, using a three-level density-matrix model, is shown in Fig. 13, where the imaginary com-

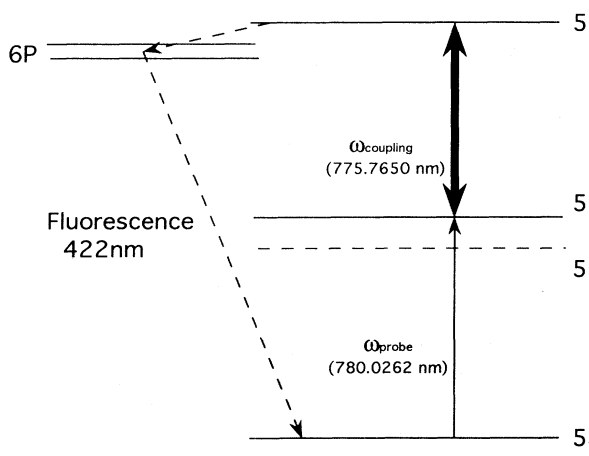

FIG. 12. Partial energy-level diagram of rubidium showing the scheme employed for the cascade system experiment.

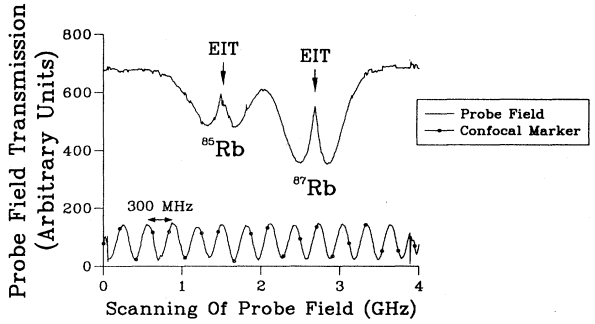

FIG. 14. Probe field transmission curve recorded versus a scan of the probe field for rubidium, within the cascade system experiment. The probe field is scanned across the $5S_{1/2}(F=2)$-$5P_{3/2}$ transition for ^{87}Rb and across the $5S_{12}(F=3)$-$5P_{3/2}$ transition for ^{85}Rb, while the coupling field is resonant with the $5P_{3/2}$-$5D_{5/2}$ transition. The coupling field power is $\sim$600 mW. The frequency position of the two EIT features are marked by arrows. A 300-MHz confocal signal is also present as a frequency reference.

ponent of ρ_{12}, which is proportional to the probe field absorption, has been plotted against probe field detuning. In Fig. 14 we present an experimental trace showing EIT in the ^{87}Rb $5S_{1/2}(F=2)$-$5P_{3/2}$-$5D_{5/2}$ and ^{85}Rb $5S_{1/2}(F=3)$-$5P_{3/2}$-$5D_{5/2}$ systems. It can be seen that EIT windows of $\sim 70\%$ depth have been produced experimentally within this system. More recently we have observed improved EIT window depths, of $\sim 90\%$, in this cascade system, when the 10-cm vapor cell was replaced by a 2-cm cell [24]. Coupling field power levels and detuning effects on this EIT window have also been studied extensively in Ref. [24] and so are not reexamined here. The spatial profile of the coupling field gives rise to varying Rabi frequencies across the probe field. This accounts for electromagnetically induced focusing effects [12] and for the reduced level of transparency observed experimentally as compared with theoretical predictions that do not take this into account.

VIII. DISCUSSION

The observation of EIT is much more complicated than is suggested by theoretical modeling using ideal three-levels systems. These simple models imply that a Λ-type system should produce the best EIT while the poorest EIT occurs in the V-type system. However, many complicating factors exist in practical experiments as have been discussed above. These are found to mask the presence of EIT and so alter this ideal picture. A major complicating factor that appears in two of the above systems, but not in our cascade system, is that of optical pumping between hyperfine ground-state levels. This occurs when the coupling field is resonant with one of the ground-state levels, inducing large-scale population movement. In the Λ-type single-photon system described, this optical pumping mechanism always works against EIT. This reduces the induced transparency within the medium but allows EIT to be experimentally resolved. For the V-type system optical pumping between hyperfine levels works with EIT when present, making it impossible to resolve the EIT feature. However, if rendering the medium transparent at the probe wavelength is the desired effect, then this latter optical pumping mechanism is a favorable process. This is not the case for the second optical pumping mechanism discussed in context with the V-type system, i.e., optical pumping between ground-state magnetic hyperfine sublevels. The presence of this mechanism provides a reduced transparency feature on top of which any transparency increasing mechanisms can be observed. Within our V-type system there are always two transparency increasing mechanisms that can never the resolved completely: EIT and coupling field saturation. It should be noted that both of these mechanisms are also present along with optical pumping between hyperfine ground states, but are masked by this effect.

Another useful guide for predicting the possibility of observing EIT is the residual Doppler linewidth values. This again predicts that the Λ-type system used here should be best for the observation of EIT since the single-photon probe Λ-type system has a residual width of the order of a few kilohertz, compared with megahertz for other systems. The two-photon probe Λ-type system proved a more difficult, but not impossible, system for observing EIT because of the increase in the residual linewidths to 710 MHz. However, this system did remove the complications of optical pumping between hyperfine ground-state levels suffered by the single-photon Λ-type system. This highlights the importance of trying to find an EIT system that employs optical fields that have well-matched wavelengths and do not have the coupling field resonant with the ground state. This is exactly the case found within our cascade system. With near-wavelength-matched, counterpropagation optical fields and no large-scale optical pumping mechanisms, the cascade system proved by far the easiest system for the uncomplicated observation of EIT. This does not imply that the other systems should be totally discarded. With better matched confocal parameters and shorter cells, better EIT may be produced within either of the other two systems. However, in practice, it has proven easier to observe EIT within this cascade system. This allows detailed studies of EIT to be undertaken without the complicating factors of optical pumping and coupling field saturation.

IX. CONCLUSION

This paper has discussed the feasibility of three different systems for the observation of continuous-wave EIT. Theoretical predictions have been complemented by comparative experimental studies on all the systems. Optical pumping has been shown to mask the presence of an EIT window, particularly for the case where the coupling field is resonant with the ground state of the atomic system. A second factor that can dramatically effect the depth of an EIT window is the residual Doppler linewidth of the atomic system. To reduce the effective residual Doppler linewidths, an atomic system must be chosen such that the two applied optical fields have similar wavelengths. Also for the V-type and Λ-type systems it is important that the applied optical fields copropagate, whereas the cascade system requires a counterpropagating geometry. Taking all these factors into account, it is found that the cascade system is the least complicated to work in, producing EIT windows of some 90%. However, EIT windows were also clearly observed within the V-type and Λ-type systems.

ACKNOWLEDGMENTS

This work was funded by the Engineering and Physical Sciences Research Council (EPSRC) under Grant No. GR/H 95440. D.J.F. would like also to acknowledge EPSRC for personal financial support.

[1] A. Imamoğlu and S. E. Harris, Opt. Lett. **14**, 1344 (1989).
[2] K. J. Boller, A. Imamoğlu, and S. E. Harris, Phys. Rev. Lett. **66**, 2593 (1991).
[3] K. Hakuta, L. Marmet, and B. P. Stoicheff, Phys. Rev. Lett. **66**, 596 (1991).
[4] K. Hakuta, L. Marmet, and B. P. Stoicheff, Phys. Rev. A **45**, 5152 (1992).
[5] S. E. Harris, J. E. Field, and A. Imamoğlu, Phys. Rev. Lett. **64**, 1107 (1990).
[6] R. R. Moseley, B. D. Sinclair, and M. H. Dunn, Opt. Commun. **101**, 139 (1993).
[7] P. Mandel, Contemp. Phys. **34**, 235 (1993).
[8] M. Fleischhauer, C. H. Keitel, M. O. Scully, C. Su, B. T. Ulrich, and S. Y. Zhu, Phys. Rev. A **46**, 1468 (1992).
[9] M. O. Scully, Phys. Rep. **219**, 191 (1992).
[10] J. G. Banacloche, Y. Li, S. Jin, and M. Xiao, Phys. Rev. A **51**, 576 (1995).
[11] M. Xiao, Y. Li, S. Jin, and J. G. Banacloche, Phys. Rev. Lett. **74**, 666 (1995).
[12] R. R. Moseley, S. Shepherd, D. J. Fulton, B. D. Sinclair, and M. H. Dunn, Phys. Rev. Lett. **74**, 670 (1995).
[13] M. Jain, G. Y. Yin, J. E. Field, and S. E. Harris, Opt. Lett. **18**, 998 (1993).
[14] S. E. Harris, Phys. Rev. Lett. **70**, 552 (1993).
[15] S. E. Harris, Phys. Rev. Lett. **72**, 52 (1994).
[16] J. H. Eberly, M. L. Pons, and H. R. Haq, Phys. Rev. Lett. **72**, 56 (1994).
[17] A. Weiss, F. Sander, and S. I. Kanorsky, in *IEEE Technical Digest, 5th European Quantum Electronics Conference '94* (Optical Society of America, Washington, DC, 1994), p. 252.
[18] J. A. Kleinfeld and A. D. Streater, Phys. Rev. A **49**, R4301 (1994).
[19] H. R. Gray, R. M. Whitley, and C. R. Stroud, Jr., Opt. Lett. **3**, 218 (1978).
[20] O. A. Kocharovskaya, F. Mauri, and E. Arimondo, Opt. Commun. **84**, 393 (1991).
[21] A. D. Wison-Gordon, Phys. Rev. A **48**, 4639 (1993).
[22] A. M. Akulshin, A. A. Celikov, and V. L. Velichansky, Opt. Commun. **84**, 139 (1991).
[23] J. E. Field, K. H. Hahn, and S. E. Harris, Phys. Rev. Lett. **67**, 3062 (1991).
[24] R.R. Moseley, S. Shepherd, D. J. Fulton, B. D. Sinclair, and M. H. Dunn, Opt. Commun. (to be published).
[25] D. J. Fulton, R. R. Moseley, S. Shepherd, B. D. Sinclair, and M. H. Dunn, Opt. Commun. **116**, 231 (1995).
[26] R. G. Brewer and E. L. Hahn, Phys. Rev. A **11**, 1641 (1975).
[27] B. Shore, *The Theory of Coherent Atomic Excitation* (Wiley, New York, 1990), Vol. 2.
[28] S. Shepherd, Ph.D. thesis, University of St. Andrews, Scotland, 1993 (unpublished).
[29] W. Happer, Rev. Mod. Phys. **44**, 169 (1972).
[30] V. S. Letokhov and V. P. Chebotayev, *Nonlinear Laser Spectroscopy* (Springer-Verlag, Berlin, 1977).